

# Extended Model for Polymer Cholesteric Liquid Crystal Flake Reorientation and Relaxation

## Introduction

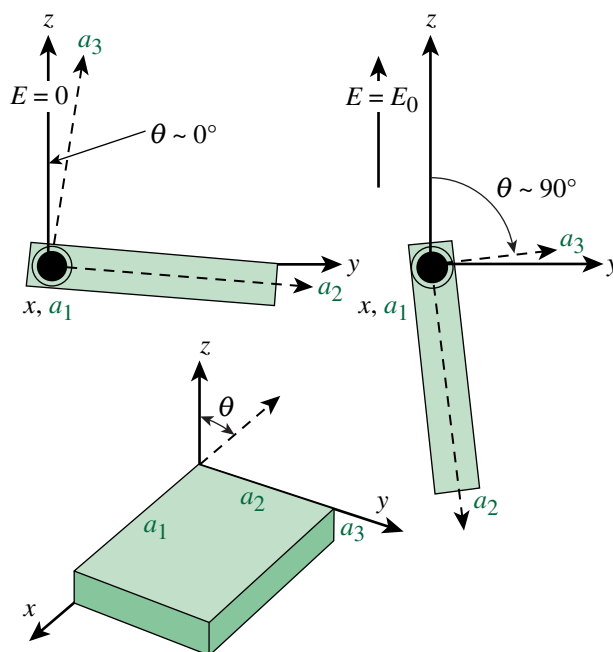
The suspension of polymer cholesteric liquid crystal (PCLC) flakes in a fluid creates the possibilities for a particle-based, electrically driven technology with a wide variety of applications ranging from displays and electronic paper to electro-optic polarizers and filters. The technology produces devices with a bright, saturated, and circularly polarized reflective “OFF” state. When an electric field, as low as tens of millivolts per micrometer, is applied, the flakes reorient at  $\sim 90^\circ$  to the electrodes, creating a dark, nonreflective “ON” state.<sup>1</sup> The PCLC flakes can be microencapsulated, and the technology is compatible with flexible substrates and roll-to-roll processing.<sup>2</sup> Originally produced by freeze-fracturing thin PCLC films,<sup>3</sup> PCLC flakes can now be manufactured with specific sizes and shapes,<sup>4</sup> altered electro-optic properties,<sup>5</sup> and enhanced reflectivity.<sup>6</sup>

The main mechanism for flake reorientation, Maxwell–Wagner polarization, is strengthened by extrinsic charges that accumulate at the surface of the flake when an electric field is applied. As these charges continue to migrate toward the edges of the flake, a dipole moment is induced. The charges responsible for the flake polarization come from ionic contaminants on and within the flakes themselves, the host fluid, and the device substrates.<sup>1</sup>

An early theoretical model for PCLC flake motion included both a hydrodynamic and an electrostatic term.<sup>1</sup> Flake rotation is taken to occur about its center of mass, so the force of gravity was not considered. This early model predicts flake reorientation well, but it has no mechanism for modeling flake *relaxation* (defined as the flake’s return to its initial position once the electric field is removed). Upon re-evaluation of the mechanics of flake rotation, it became clear that many flakes tend to rotate about a pivot point near or at their edge. This article discusses a new extended theoretical model that includes a gravity term and presents experimental data that support this extended model. Both reorientation (torques caused by electric-field, viscous flow, and gravity present) and relaxation (viscous and gravity torques only) are discussed.

## Theory

Previously, we described the derivation of a theoretical model that assumes a PCLC flake subjected to an external electric field will reorient about its center of mass and along its longest axis  $a_1$  with a negligible moment of inertia.<sup>1</sup> This configuration leads to the inclusion of only the electrostatic  $\Gamma_E$  and hydrodynamic  $\Gamma_H$  torques because gravity, which acts on the center of mass, would not affect motion. A series of experiments showed that flakes often reorient about the edge of their longest side (Fig. 118.23).



G8678JR

Figure 118.23

A two-dimensional cross-sectional depiction of a PCLC flake with its semi-axes defined as  $a_1 > a_2 > a_3$ . The electric field is applied along the  $z$  axis. Modeling presumes a particle position is (a) at  $\theta \sim 0^\circ$  for  $E = 0$  and (b) at  $\theta \sim 90^\circ$  for  $E = E_0$ .

Rotation about a flake’s edge makes the torque caused by gravity,  $\Gamma_G$ , relevant to the equation of motion governing flake behavior and extends the theoretical model to describe reorientation as

$$\Gamma_E - \Gamma_H - \Gamma_G = 0. \quad (1)$$

The electrostatic torque about the  $a_i$  axis, which drives flake reorientation, is given as

$$\begin{aligned} \Gamma_{Ei} &= \frac{4}{3} \pi a_i a_j a_k \varepsilon_h K_j^* K_k^* (A_k - A_j) E_{0j} E_{0k} \\ &= C_{Ei} \sin \theta \cos \theta, \end{aligned} \quad (2)$$

where  $E_0$  is the electric-field magnitude,  $E_{0j} = E_0 \sin \theta$  and  $E_{0k} = E_0 \cos \theta$  are projections of an electric field applied in the  $z$  direction.<sup>7</sup> The lengths of the particle semi-axes are designated as  $a_i$ ,  $a_j$ , and  $a_k$ , and a depolarization factor  $A_i$  is defined along each axis. The indices  $i$ ,  $j$ , and  $k$  are ordered according to the right-hand coordinate system. To find  $A_j$ , assign  $i \rightarrow j$ ,  $j \rightarrow k$ , and  $k \rightarrow i$ ;  $s$  is a symbolic variable in the elliptical integral.

$$A_i = \frac{a_i a_j a_k}{2} \int_0^\infty \frac{ds}{(s + a_i^2) \sqrt{(s + a_i^2)(s + a_j^2)(s + a_k^2)}}. \quad (2a)$$

The complex Clausius–Mossotti function  $K_i^*$  is defined as

$$K_i^* = \frac{\left( \varepsilon_p - i \frac{\sigma_p}{\omega} \right) - \left( \varepsilon_h - i \frac{\sigma_h}{\omega} \right)}{\left( \varepsilon_h - i \frac{\sigma_h}{\omega} \right) + A_i \left[ \left( \varepsilon_p - i \frac{\sigma_p}{\omega} \right) - \left( \varepsilon_h - i \frac{\sigma_h}{\omega} \right) \right]}. \quad (2b)$$

The dielectric permittivity and conductivity of the host fluid,  $\varepsilon_h$  and  $\sigma_h$ ; the particles,  $\varepsilon_p$  and  $\sigma_p$ ; and the electric-field frequency  $\omega$  are the main parameters in the Clausius–Mossotti term. The constant  $C_{Ei}$  contains all parameters in the electrostatic torque term. The electrostatic term is complex because of the inclusion of the material conductivities. The hydrodynamic torque counteracts the electrical torque,

$$\Gamma_{Hi} = \frac{16}{3} \pi a_i a_j a_k \eta_0 \frac{(a_j^2 + a_k^2)}{(a_j^2 A_j + a_k^2 A_k)} \Omega_i = C_{Hi} \Omega_i, \quad (3)$$

where  $\eta_0$  is the fluid viscosity,  $\Omega_i$  is the angular velocity about axis  $i$ , and  $C_{Hi}$  is a constant including all other parameters. The gravitational torque is found to be

$$\Gamma_{Gi} = \frac{4}{3} \pi a_i a_j a_k (\rho_p - \rho_h) g a_j \cos \theta = C_{Gi} \cos \theta, \quad (4)$$

where  $\rho_p$  and  $\rho_h$  are the density of the particle and the host fluid, respectively,  $g$  is the acceleration of gravity, and  $C_{Gi}$  is a constant including related gravity-term parameters. For very small applied electric fields, the electrical torque term  $\Gamma_E$  would no longer be able to overcome the gravity term  $\Gamma_G$  and flake reorientation would not occur. Because the condition under which flakes do not reorient was not relevant to this work, the minimum effective electric field was not investigated.

### 1. Reorientation Time

The time required for a flake to reorient from an initial position at the angle  $\theta_0$  to its final position at  $\theta_f$  is found by rearranging the equation of motion to define the angular velocity along the axis  $a_i$ :

$$\Omega_i = \frac{d\theta}{dt} = \frac{\cos \theta (C_{Ei} \sin \theta - C_{Gi})}{C_{Hi}}. \quad (5)$$

Equation (5) is then integrated to find the reorientation time  $t$  required to attain the angle  $\theta_f$  from the flake's initial position at angle  $\theta_0$ :

$$t = \frac{C_{Hi}}{C_{Ei}^2 - C_{Gi}^2} \left\{ \begin{aligned} & \left[ (C_{Gi} - C_{Ei}) \ln \left[ \cos \left( \frac{\theta}{2} \right) + \sin \left( \frac{\theta}{2} \right) \right] \right]_{\theta_0}^{\theta_f} \\ & - (C_{Ei} + C_{Gi}) \ln \left[ \cos \left( \frac{\theta}{2} \right) - \sin \left( \frac{\theta}{2} \right) \right] \\ & + C_{Ei} \ln [C_{Gi} - C_{Ei} \sin(\theta)] \end{aligned} \right\}. \quad (6)$$

The inclusion of the gravity term makes the resulting equation for reorientation time more complicated. The linear dependence of the host fluid's viscosity is retained, but the electric field's dependence is no longer inversely quadratic and it varies depending on system parameters. Although it is common to use the real component of the equation when the modeled motion is much slower than the electric-field oscillation, we have shown previously that, using the real component poorly predicts the reorientation time as a function of electric-field frequency.<sup>1</sup> A remarkably closer agreement with experimental data is achieved by using the imaginary component, although no clear physical interpretation for this term has been proposed.

The extended model is used to calculate the reorientation time as a function of frequency (Fig. 118.24) for the newly introduced variable (the host fluid's density), ranging in value

from 900 to 1300 kg/m<sup>3</sup>. For the calculation, the PCLC particle density is fixed at 1101 kg/m<sup>3</sup>, and all other host fluid properties are based on those for propylene carbonate. When the particle and fluid densities are matched, the gravity term vanishes, resulting in the same predictions as the initial theory (dotted line in Fig. 118.24). The electrostatic torque diminishes and reorientation times steadily increase toward infinity as the electric-field frequency shifts up or down from its optimal value for flake reorientation time.

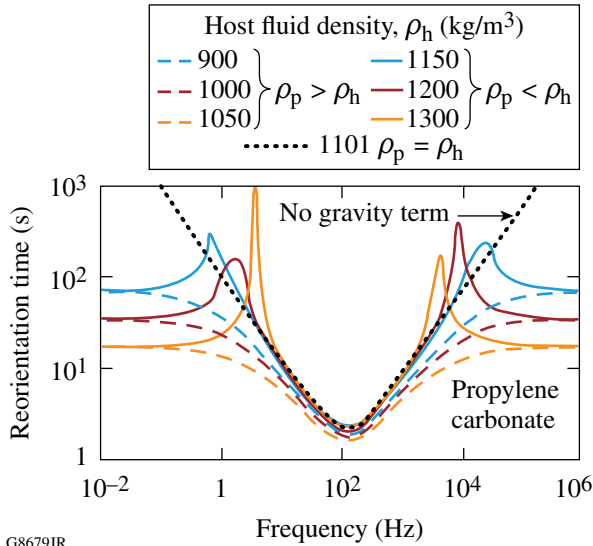


Figure 118.24

The reorientation time of a typical flake ( $\rho_p = 1099 \text{ kg/m}^3$ ,  $\epsilon_p = 2.98$ , and  $\sigma_p = 10^{-10} \text{ S/m}$ ) suspended in a fluid with the base properties of propylene carbonate ( $\epsilon_h = 69$ ,  $\sigma_h = 10^{-7} \text{ S/m}$ , and  $\eta_0 = 2.8 \times 10^{-3} \text{ N} \times \text{s/m}^2$ ) is examined as a function of the density of the host fluid,  $\rho_h$ . Particle semi-axes are  $a_1 = 30 \text{ } \mu\text{m}$ ,  $a_2 = 20 \text{ } \mu\text{m}$ , and  $a_3 = 2 \text{ } \mu\text{m}$ . The orientation angles  $\theta_0 = 0.5^\circ$  and  $\theta_f = 89.5^\circ$  are used to avoid singularities in applying Eq. (6).

The effect of the gravity term grows as the difference between the flake and the fluid density increases. When the particle density is *greater* than that of the host fluid ( $\rho_p > \rho_h$ ), the extended theory predicts faster reorientation times (dashed lines in Fig. 118.24) than those predicted by the original theory. This result suggests that the gravity term is additive to the electrostatic torque driving flake reorientation. The reorientation times based on the extended model no longer increase toward infinity, as originally predicted. Instead, reorientation times at both extremes of the frequency range asymptote to a value equal to the ratio of the hydrodynamic term to the gravity term. The asymptotic value decreases as the host fluid density decreases and the difference between particle density and host fluid density grows.

The extended theory predicts a more-complicated frequency response when the density of the particle is *less* than that of the host fluid ( $\rho_p < \rho_h$ ). Reorientation times near the curve minimum are predicted by the extended theory to be slightly lower. Outside this range, however, the gravity term *counteracts* the electrostatic term. Flake reorientation times start to *increase*, forming a peak when the contributions of the electrostatic and gravity terms lead toward canceling each other in the denominator of Eq. (6). When the electrostatic torque becomes negligible compared to the magnitude of the gravity term, the ratio of the hydrodynamic term to the gravity term once again defines the value of the reorientation times. At very low and very high frequencies, the reorientation time asymptotes to the same value for systems with the same absolute difference between particle and host fluid densities.

Depending on both the frequency of the applied electric field and the density of the host fluid, the gravity term either enhances or counteracts the electrostatic torque that is driving flake motion. Using propylene carbonate ( $\rho_p < \rho_h$ ), it is possible to study how the relative strength of the electrostatic torque influences the shape of the predicted frequency response. The model is exercised with the same material parameters noted above, and the driving voltage is varied from 12.5 to 31.1 mV<sub>rms</sub>/μm. The results show that higher driving voltages result in faster reorientation times over a broadening range of frequencies (see Fig. 118.25). Again, reorientation times at the frequency extremes asymptote to a value dictated by the ratio of the hydrodynamic and gravity terms. As the magnitude of the electrostatic torque diminishes with lower applied voltages,

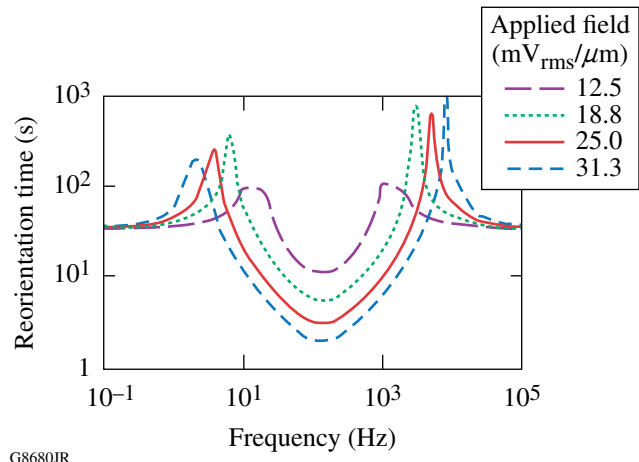


Figure 118.25

The reorientation time of a PCLC flake suspended in propylene carbonate ( $\rho_p < \rho_h = 1200 \text{ kg/m}^3$ ) is examined as a function of driving voltage.

the extended model shows how the gravity term increasingly influences flake motion. As the electrostatic torque diminishes, it eventually cannot overcome gravity. For the condition where  $\Gamma_E \sim \Gamma_G$ , the reorientation time will approach infinity.

## 2. Relaxation Time

The inclusion of the gravity term in Eq. (1) provides a driving mechanism for motion of a reoriented flake when the electric field is removed, and it becomes possible to calculate the relaxation time  $t_{\text{relax}}$ . The relaxation time is defined as the time required for a flake to return from its “reoriented” position (typically  $\theta_0 \sim 90^\circ$ ) to its original position ( $\theta_f \sim 0^\circ$ ) once the electric field has been removed (Fig. 118.23 depicts a view of flake position). The hydrodynamic and the gravity terms are equated and, following the same procedure described previously, the relaxation time is determined:

$$t_{\text{relax},i} = \frac{4\eta_0 \frac{(a_j^2 + a_k^2)}{(a_j^2 A_j + a_k^2 A_k)}}{|\rho_p - \rho_h| g a_j} \ln \left( \frac{1 + \sin \theta}{\cos \theta} \right)_{\theta_0}^{\theta_f}. \quad (7)$$

The relaxation time has a linear dependence on the host fluid’s viscosity and an inverse dependence on the absolute difference between material densities. The flake’s shape and orientation (with respect to the direction of gravity) also influence relaxation. When the density of the host fluid and the flake are matched, the relaxation time increases to infinity. Otherwise, the change in relaxation time is symmetric, decreasing as the absolute difference in densities between the two media increases. A comparison of the predicted relaxation times is given with experimental results in **Relaxation Time** (p. 84).

## Experimental

The validity of the extended model is examined with experimental data for both reorientation and relaxation times of various PCLC flakes. Particle reorientation is observed in the standard particle/host fluid system of PCLC flakes suspended in propylene carbonate. Relaxation times are acquired for flakes suspended in various host fluids, so that the effect of the host fluid’s density and viscosity can be studied.

### 1. Reorientation Time

The behavior of commercially produced, randomly shaped and sized polysiloxane PCLC flakes<sup>8</sup> in propylene carbonate is reproducible and well-documented.<sup>1</sup> Reorientation-time data presented by Kosci *et al.* were analyzed again and are shown in Fig. 118.26. PCLC flake reorientation was observed in a 44- $\mu\text{m}$

cell gap at four driving voltages over a nearly three decade frequency range. The original gravity-free model (dashed lines) predicts reorientation times well. The extended theory continues to produce a good fit for some of the experimental data. This new model predicts vertical asymptotes at two specific frequencies, a feature that appears to coincide with the frequency band for which flake reorientation is experimentally observed at high driving fields. However, as the driving fields become lower, the extended model predicts longer reorientation times than those observed experimentally. Furthermore, the data no longer fit neatly within the frequency band between the vertical asymptotes or follow the asymptotes. This result suggests that, as the magnitude of the electrical torque diminishes, there is still some factor or effect that counteracts the gravity term and does not allow it to dominate as strongly as the extended theory predicts. Such a term may be related to the way in which the hydrodynamic torque term is utilized. The implicit assumption of steady rotation is not necessarily valid in the context of the obvious time-dependent rotation of the flake in the confine of space between the two electrodes. A similar observation can be made about the dependence of the hydrodynamic torque on the flake angle: one would expect that a flake parallel to the electrode would experience a different torque from the flake perpendicular to the electrodes when the electrode gap is comparable to the flake dimension; however, neither flake acceleration nor flake proximity to electrodes is considered in the theory.

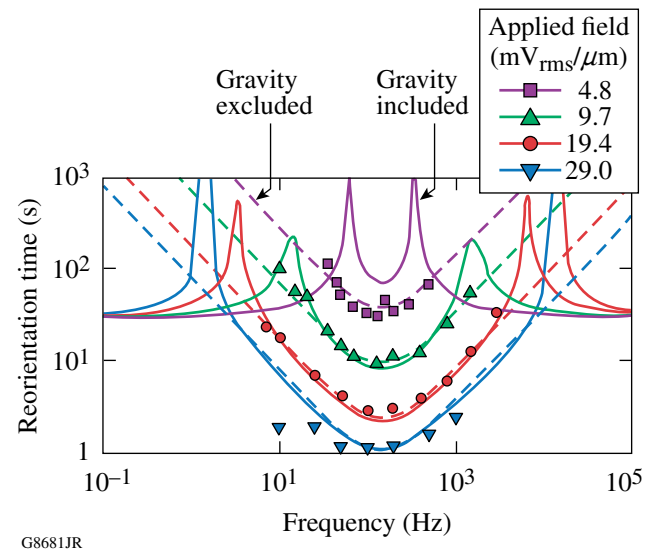


Figure 118.26  
The reorientation times of a representative PCLC flake (semi-axes are  $a_1 = 17.5 \mu\text{m}$ ,  $a_2 = 7.6 \mu\text{m}$ , and  $a_3 = 2.5 \mu\text{m}$ ) suspended in propylene carbonate ( $\rho_p < \rho_h$ ) are compared with the theoretical fit predicted by the original model (dashed lines) and the extended model (solid lines).

## 2. Relaxation Time

The relaxation time  $t_{\text{relax}}$  of flakes is investigated by suspending uniformly shaped and sized polysiloxane PCLC flakes manufactured in-house<sup>4</sup> in nine host fluids, including blends of propylene carbonate (PC) and the silicone oil E09, gamma-butyrolactone (GBL), and ethylene glycol (EG) (Table 118.I). The densities and viscosities of neat (pure) fluids are tabulated from vendor literature. The density and viscosity values for the PC/E09 blends are based on use of the additivity law of mixtures (volume ratio is used) and literature values for the neat fluids.

Table 118.I: Properties of experimental neat and blended host fluids used for modeling are listed in order of decreasing density of the host fluid. The polysiloxane PCLC material is placed in the table for reference. Pure fluids are given in shadowed rows.

PC/E09	$\rho_h$ (kg/m <sup>3</sup> ) at 20°C	$\eta_0$ (mPa • s) at 20°C	Relaxation time (min)
PC (Ref. 9)	1200	2.8	50 s
71/29	1141	5.2	2
GBL (Ref. 10)	1128	1.9	2
EG (Ref. 11)	1112	18	37
57/43	1112	6.3	12
54.5/45.5	1107	6.5	3
PCLC	1101	/	/
50/50	1098	6.9	15
33/67	1063	8.3	3
E09 (Ref. 12)	995*	11.0*	3

\*Vendor data acquired at 25°C.

For all systems, the flakes are reoriented with an applied electric field of 40 mV<sub>rms</sub>/μm, and the relaxation time is determined by measuring the time required for the flake to return to its original position once the driving field has been removed. Because the relaxation time is linearly dependent on the viscosity  $\eta_0$  and the difference between the particle and host fluid density ( $\rho_p - \rho_h$ ), the effect of both parameters can be considered independently. Both the densities and viscosities of these materials are temperature dependent. This temperature dependence introduces some uncertainty into the results because experiments are conducted at temperatures between 20°C and 23°C. Furthermore, the given relaxation times are a best estimate from observations of several flakes. Flake properties such as thickness and density are prone to variation because of their laboratory-based manufacturing process. Slight variations in these flake properties were most significant for systems

where the host fluid's density was nearly matched with that of the PCLC flake or where the fluid viscosity was high, which for both cases results in long relaxation times.

To examine the effect of fluid density independent of fluid viscosity, the experimental and theoretical relaxation time data are divided by the fluid viscosity [Fig. 118.27(a)]. The predicted relaxation times show the easily recognizable inverse dependence on the  $(\rho_p - \rho_h)$  term in the denominator of Eq. (7). The experimental data agree well with the model, and flakes relax most quickly when the absolute magnitude of the difference between particle and fluid densities is the greatest. As the host fluid density of the PC/E09 mixtures approaches that of the PCLC flake, the relaxation times increase considerably. A similar analysis is performed to study the effect of the host fluid's viscosity. As shown in Fig. 118.27(b), the experimental data agree well with the predicted linear dependence of flake relaxation on fluid viscosity.

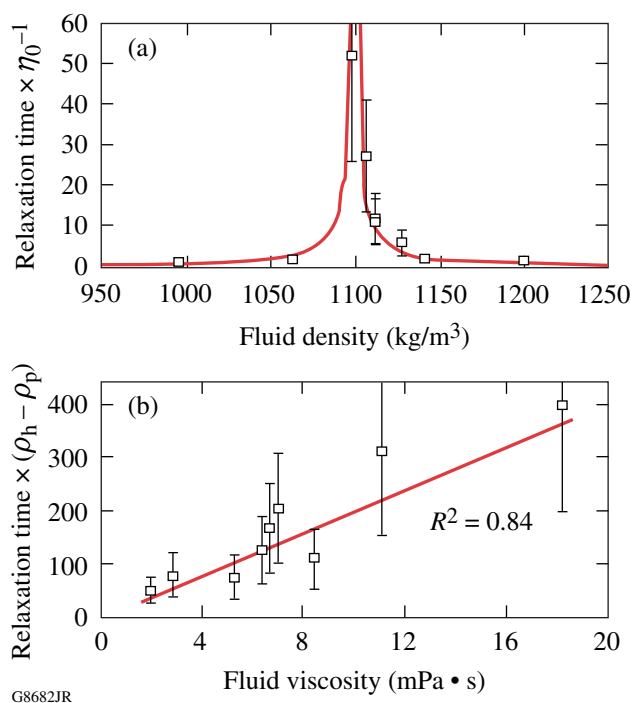


Figure 118.27

Relaxation times of a PCLC flake (semi-axes are  $a_1 = 30 \mu\text{m}$ ,  $a_2 = 10 \mu\text{m}$ , and  $a_3 = 2 \mu\text{m}$ ) suspended in various host fluids are compared with the theoretical fit as a function of host fluid's (a) density and (b) viscosity. Error bars of 50% have been ascribed to the data.

## Summary and Conclusions

The modeling of PCLC flake motion has been extended to include the effect of gravity in addition to the electrostatic

and hydrodynamic terms. The gravity term introduces vertical asymptotes, which, for high driving fields, appear to provide a boundary for the general frequency range in which flake motion is observed. For lower electric-field values, however, the model fit to the experimental data degrades, suggesting that additional terms might be needed to complete the model. The inclusion of the gravity term in the extended model provides, for the first time, a driving mechanism for modeling flake relaxation. Theory and experiment agree well in the demonstration of the relaxation time's linear dependence on the fluid viscosity and inverse dependence on the density difference between materials.

#### ACKNOWLEDGMENT

The authors would like to acknowledge the Laboratory for Laser Energetics at the University of Rochester for continuing support. This work was also supported by the U.S. Department of Energy Office of Inertial Confinement Fusion under Cooperative Agreement No. DE-FC52-08NA28302, the University of Rochester, and the New York State Energy Research and Development Authority. The support of DOE does not constitute an endorsement by DOE of the views expressed in this article.

#### REFERENCES

1. T. Z. Kosc, K. L. Marshall, S. D. Jacobs, and J. C. Lambropoulos, *J. Appl. Phys.* **98**, 013509 (2005).
2. G. P. Cox, K. L. Marshall, M. Leitch, C. Fromen, T. Knab, D. Berman, and S. D. Jacobs "Modeling Microencapsulation Effects on the Electro-Optic Behavior of Polymer Cholesteric Liquid Crystal Flakes," submitted to *Advanced Functional Materials*.
3. E. M. Korenic, S. D. Jacobs, S. M. Faris, and L. Li, *Mol. Cryst. Liq. Cryst.* **317**, 197 (1998).
4. A. Trajkovska-Petkoska, R. Varshneya, T. Z. Kosc, K. L. Marshall, and S. D. Jacobs, *Adv. Funct. Mater.* **15**, 217 (2004).
5. A. Trajkovska Petkoska and S. D. Jacobs, *Mol. Cryst. Liq. Cryst.* **495**, 334 (2008).
6. K. L. Marshall, K. Hasman, M. Leitch, G. Cox, T. Z. Kosc, A. Trajkovska-Petkoska, and S. D. Jacobs, in *2007 SID International Symposium*, edited by J. Morreale (Society for Information Display, San Jose, CA, 2007), Vol. XXXVIII, Book II, pp. 1741–1744.
7. T. B. Jones, *Electromechanics of Particles* (Cambridge University Press, New York, 1995).
8. Wacker-Chemie, Consortium für Electrochemische Industrie GmbH, Zielstattstrasse 20, D-81379 München, Germany.
9. C. M. Hansen, *Hansen Solubility Parameters: A User's Handbook*, 2nd ed. (CRC Press, Boca Raton, FL, 2007), p. 129.
10. Technical Leaflet, BASF Aktiengesellschaft, 67056 Ludwigshafen, Germany (2006).
11. Engineers Edge, Monroe, GA 30656. See [http://www.engineersedge.com/fluid\\_flow\\_data.htm](http://www.engineersedge.com/fluid_flow_data.htm) (2009).
12. Gelest, Inc., Morrisville, PA 19067.